Q. J. R. Meteorol. Soc. (2004), **128**, pp. 1–999 doi: 10.1256/qj.

Note on the effect of horizontal gradients for nadir-viewing microwave and infrared sounders

By J. JOINER[1]*, P. POLI[2,3,4]

[1]*NASA Goddard Space Flight Center Laboratory for Atmospheres, USA*
[2]*University of Maryland, Baltimore County, USA*
[3]*Centre National de Recherches Météorologiques, Météo France, Toulouse, France*
[4]*NASA Goddard Space Flight Center Global Modeling and Assimilation Office*

(Received 1 January 2004; revised 31 January 2004)

SUMMARY

Passive microwave and infrared nadir sounders such as the Advanced Microwave Sounding Unit A (AMSU-A) and the Atmospheric InfraRed Sounder (AIRS), both flying on NASA's EOS Aqua satellite, provide information about vertical temperature and humidity structure that is used in data assimilation systems for numerical weather prediction and climate applications. These instruments scan cross track so that at the satellite swath edges, the satellite zenith angles can reach ~60°. The emission path through the atmosphere as observed by the satellite is therefore slanted with respect to the satellite footprint's zenith. Although radiative transfer codes currently in use at operational centers use the appropriate satellite zenith angle to compute brightness temperature, the input atmospheric fields are those from the vertical profile above the center of the satellite footprint. If horizontal gradients are present in the atmospheric fields, the use of a vertical atmospheric profile may produce an error.

This note attempts to quantify the effects of horizontal gradients on AIRS and AMSU-A channels by computing brightness temperatures with accurate slanted atmospheric profiles. We use slanted temperature, water vapor, and ozone fields from data assimilation systems. We compare the calculated slanted and vertical brightness temperatures with AIRS and AMSU-A observations. We show that the effects of horizontal gradients on these sounders are generally small and below instrument noise. However, there are cases where the effects are greater than the instrument noise and may produce erroneous increments in an assimilation system. The majority of the affected channels have weighting functions that peak in the upper troposphere (water vapor sensitive channels) and above (temperature sensitive channels) and are unlikely to significantly impact tropospheric numerical weather prediction. However, the errors could be significant for other applications such as stratospheric analysis. Gradients in ozone and tropospheric temperature appear to be well captured by the analyses. In contrast, gradients in upper stratospheric and mesospheric temperature as well as upper tropospheric humidity are less well captured. This is likely due in part to a lack of data to specify these fields accurately in the analyses. Advanced new sounders, like AIRS, may help to better specify these fields in the future.

KEYWORDS: assimilation AIRS AMSU radiances

1. INTRODUCTION

The Atmospheric InfraRed Sounding (AIRS) and the Advanced Microwave Sounding Unit-A (AMSU-A) (Aumann *et al.* 2003) are nadir-viewing passive sounders currently flying on the National Aeronautics and Space Administration's (NASA) Earth Observing System (EOS) Aqua platform. AMSU-A also flies on the National Oceanic and Atmospheric Administration (NOAA) Polar Orbiting Environmental Satellites (POES) along with the High-resolution InfraRed Sounder (HIRS). These and other similar sounders are the primary satellite instruments used in atmospheric data assimilation systems (DAS) for numerical weather prediction and the production of climate data sets.

Fast radiative transfer models are used to compute brightness temperatures from background fields in a DAS. Analysis increments are then generated based on the difference between the observed and the computed brightness temperatures. The effects of so-called limb-brightening or limb-darkening along a satellite scan line are accounted for in the radiative transfer model by using an appropriate satellite zenith angle. However, the input atmospheric profile is usually the

* Corresponding author: NASA Goddard Space Flight Center, Code 916, Greenbelt, MD, 20771, USA.

vertical one above the satellite footprint center. The correct atmospheric profile should also account for the fact that the emission path through the atmospheric is slanted with respect to the footprint zenith. If horizontal gradients are present, an error may occur if the vertical atmospheric path is used.

Horizontal gradient effects are a well known problem for limb-viewing sounders. For example, gradient effects have been shown to be important for the limb-viewing Global Positioning Satellite Radio Occultation sounding technique (*e.g.*, Poli and Joiner 2004; Poli 2004). The effects of horizontal gradients on nadir sounders have not be documented recently.

Over the past two decades, the amount of computing power has increased dramatically and with it the resolution of models and analysis systems. With horizontal resolutions now at the scale of tens of km even for global models, gradient effects may be significant for nadir sounders. This may be especially true for advanced high-spectral resolution sounders that have channels with high-altitude weighting function peaks. Here, we use analysed fields of temperature, humidity, and ozone from current data assimilation systems along with appropriate geometrical emission paths to accurately assess the effects of horizontal gradients for AIRS and AMSU-A.

Sections 2-5 describe the geometry, observations, background fields, and methodology, respectively, that are used to compute brightness temperatures using vertical and slanted atmospheric emission paths. In section 6 we apply the methodology to AIRS and AMSU-A channels and use observations to assess the accuracy of the gradients in the assimilated atmospheric fields. Conclusions and suggestions for further research are given in section 7.

2. Emission path geometry

Figure 1 shows the geometry for nadir and off-nadir pixels. For the off-nadir pixel with a zenith angle α and an emission height dz, there will be an offset dx in the emission path with respect to the vertical. The usual approach to calculate a radiance from a three-dimensional field at the off-nadir pixel ignores that offset. Instead, one extracts temperature and constituent (humidity, ozone) information located at the vertical above the off-nadir pixel.

In order to calculate the radiance along the slanted line-of-sight, we need to extract the information from the analysed fields along that line. The positions of the points to consider along that line are given by applying a rotation in the plane determined by the local center of curvature and the satellite azimuth angle. The angle of the rotation θ is shown in Figure 1 and can be found using simple geometry.

The offset dx can be written as $dx = dz \cdot \tan\alpha$ and is shown in Figure 2 for various altitudes dz. That distance dx has to be compared with the horizontal resolution of the analysed fields at hand (approximately 100 km or better in the tropics and higher resolution at high latitudes). For heights below 10 km, we observe that the distance dx remains below 10 km even for the largest zenith angles. Consequently, we do not expect to see much difference between slanted and vertical radiative transfer calculations for channels peaking in the lower troposphere. However, for heights of 20 km or above, offsets dx larger than 20 km are obtained for all zenith angles greater than 30 degrees. This suggests that significant brightness temperature differences may be observed for upper

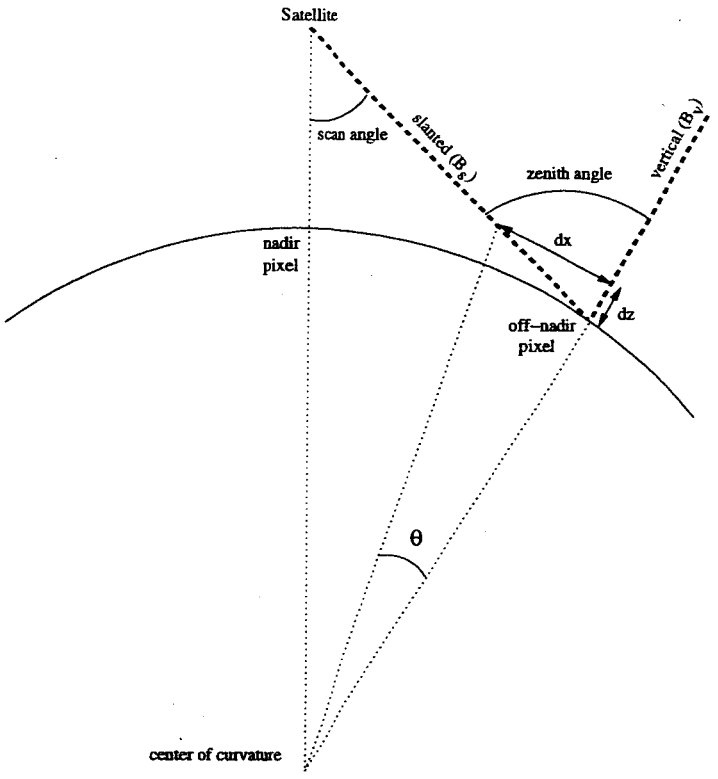

Figure 1. Schematic of AIRS footprints for nadir (left) and off-nadir (right) where dx is the offset from the center of the footprint to the actual atmospheric location of the emission path at height dz.

tropospheric and stratospheric channels when using either a vertical or slanted atmospheric profile.

3. Observations

The Aqua satellite was launched in May 2002. Here we use observations (O) from a single day (16 December 2002). We use a reduced AIRS radiance data set (Goldberg *et al.* 2003) provided by the NOAA National Environmental Satellite Data and Information Service (NESDIS). This data set contains a 281 channel subset of the 2378 available AIRS channels. We use only AMSU-A channels 3-14 that have a significant atmospheric contribution.

There are nine AIRS pixels within an AMSU-A footprint. For this study, we first select a single AIRS pixel within the AMSU-A footprint with the warmest temperature in an 11 μm window channel. We then apply the cloud detection algorithm of Joiner *et al.* (2004) to remove cloud-contaminated pixels.

4. Assimilated background fields

The background fields (B) used here come from a combination of assimilation systems. In the troposphere and lower stratosphere, temperature and humidity are from the Spectral Statistical Interpolation (SSI) analysis of the National

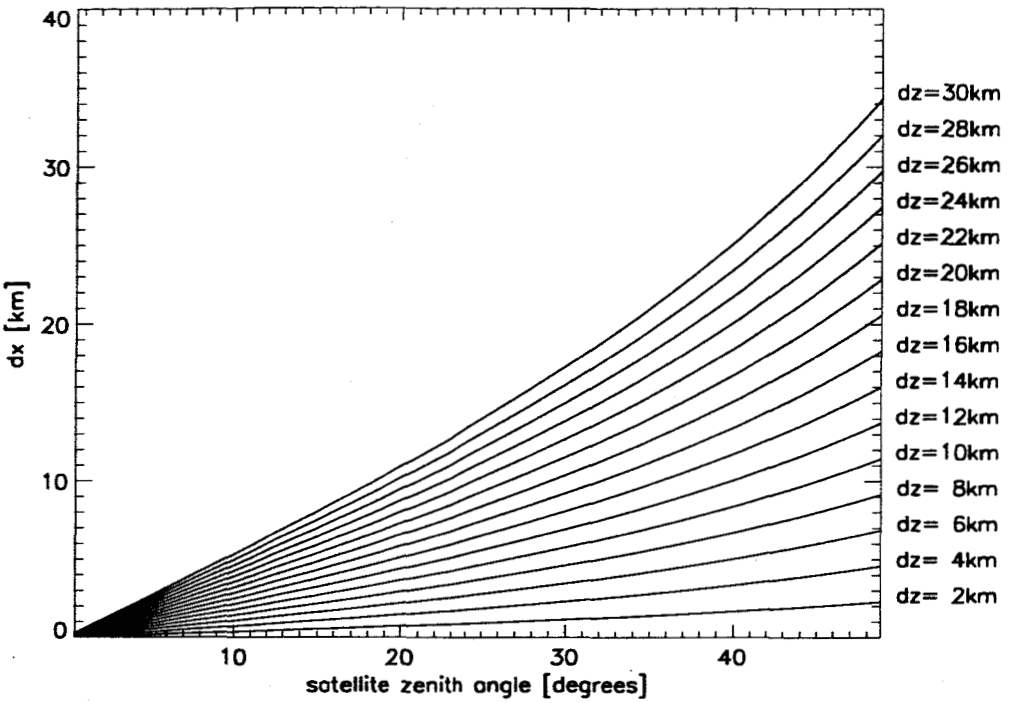

Figure 2. Horizontal offset (dx) from the center of the footprint for off-nadir pixels versus satellite zenith angle for different emission heights.

Center for Environmental Prediction (NCEP) (Derber and Wu 1998). We used the operational fields (T254L64) with a model top at 2hPa.

In the middle stratosphere and above, temperature and humidity are from a 6-hour forecast of the NASA Global Modeling and Assimilation Office (GMAO) finite volume data assimilation system. GMAO fields have a horizontal resolution of $1° \times 1°$, a model top of 0.01hPa. The general circulation model used for the GMAO DAS forecast includes the dynamical core of Lin (1997) with NCAR CCM3 physics (Kiehl *et al.* 1996). The GMAO analysis uses the Physical-Space Statistical Analysis System (PSAS) (Cohn *et al.* 1998).

The ozone fields come from an PSAS off-line analysis with a horizontal resolution of $1° \times 1°$ (Stajner *et al.* 2001). Assimilated observations were from the Solar Backscatter Ultraviolet (SBUV) radiometer.

Temperature and humidity from the NCEP and GMAO fields were combined as follows (L. Takacs, *private communication*): The NCEP spectral analysis below 10 hPa was remapped to the GMAO grid-point resolution. The remapping algorithm was designed to conserve the vertically integrated column mean of the remapped variable. Above 5 hPa, only the GMAO 6-hour forecast was used. Between 5 and 10 hPa, we used a linear blend of the GMAO first guess with the remapped NCEP analysis. This blending was designed to provide accurate fields in both the troposphere and upper stratosphere to mesosphere.

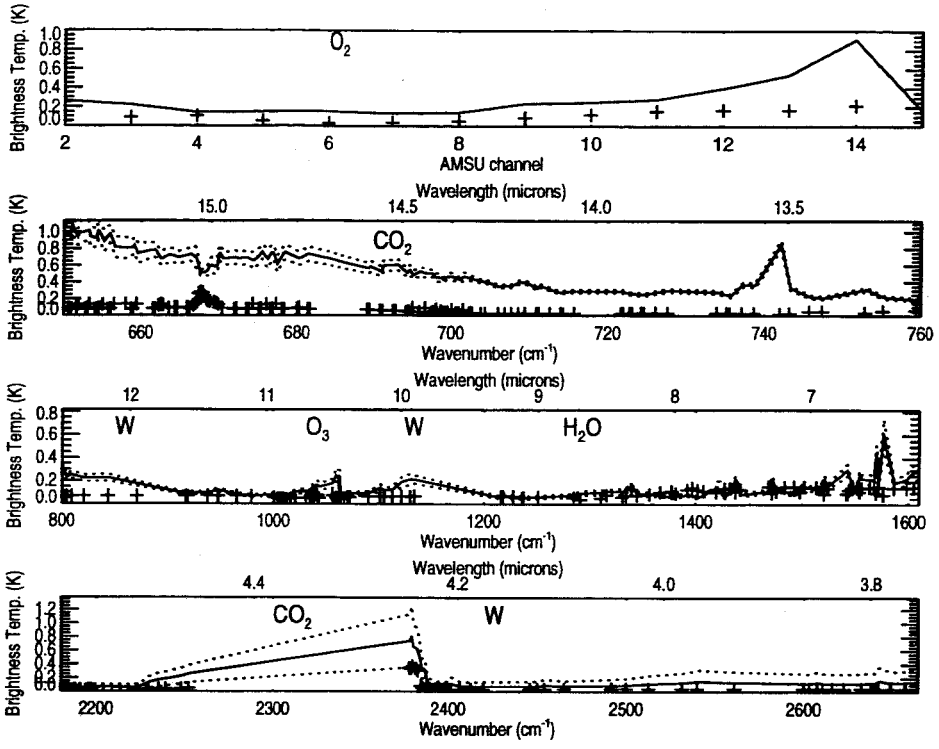

Figure 3. +: 1 σ of ΔB for AMSU-A channels (top panel) and AIRS channels (bottom 3 panels); Solid (dotted) lines: average ($\pm 1\sigma$) of the instrument noise (NEΔT), see text for explanation; Major absorption bands are indicated above with window regions denoted by 'W'.

temperature-sensitive channels in the 15μm and 4μm bands are concentrated in the northern hemisphere at middle to high latitudes where there are substantial temperature gradients. Profiles that produce the largest differences in upper tropospheric humidity channels are scattered mainly throughout the tropics.

Figure 5 shows the mean value of $\Delta|O-B|$ for each channel. Degradations (negative values) can be seen in the very high peaking temperature sounding (CO_2) channels in the 15 μm and 4μm bands. These channels are sensitive to temperatures at altitudes above the highest analysis level (0.4 hPa). Above this level, the atmospheric fields are those given by the GMAO forecast forced from below by observations primarily from the NOAA operational AMSU-A instruments (note that Aqua AMSU-A data were not assimilated in the fields used here). The negative values for these channels suggests that the temperature gradients at these altitudes in the background field may contain errors.

Similarly, we observe negative values of the mean $\Delta|O-B|$ for the highest peaking water vapor channels in the 6.7μm band. The water vapor data in the upper troposphere used in the NCEP analysis comes primarily from HIRS channel 12. The weighting function of this channel peaks below the most absorbing AIRS water vapor channels. Therefore, the data going into the analysis may not be good enough to provide information on the gradients in water vapor occurring in the upper troposphere at altitudes where the highly absorbing AIRS channel weighting functions peak.

5. Observed minus background (O-B) calculations

We use the stand-alone AIRS radiative transfer algorithm (SARTA) (Strow *et al.* 2003) to compute brightness temperatures from background fields for AIRS. We use the radiative transfer algorithm of Rosenkrantz (2003) for AMSU-A channels. We then subtract the computed background brightness temperatures from the observations. As described in Joiner *et al.* (2004) we apply systematic error correction (tuning) to correct for biases in the observations and/or forward model.

We calculate two types of differences between brightness temperatures produced using the vertical and slanted atmospheric paths. The first differences is simply the difference between the calculated brightness temperatures using the background fields with the vertical (B_v) and slanted (B_s) atmospheres, denoted ΔB. The second difference, $\Delta|O-B| = |O-B_v| - |O-B_s|$, is a designed to assess whether the use of the slanted atmospheric path improves upon the use of the vertical path. A positive (negative) value of $\Delta|O-B|$ denotes an improvement (degradation) of the computed brightness temperature by using the slanted path compared with that using the vertical path as measured by the distance from the observation.

6. Results obtained with AIRS and AMSU-A data

In this section, all results will be restricted to observations with satellite zenith angles greater than 50°. Figure 3 shows the channel standard deviations of the brightness temperature differences between calculations using vertical and slanted atmospheres (ΔB). For reference, we also show the detector noise values in terms of noise-equivalent temperature (NEΔT). For AIRS channels, we took the reported NEΔT values at a reference temperature of 250 K (S. Y. Lee, *private communication*) and computed a value of NEΔT at each cloud-free observed brightness temperature. The solid line is the average value of NEΔT for each channel and the dotted lines are the average $\pm$ 1σ. For most channels, the standard deviations of ΔB are well below the detector noise. However, they are comparable to the noise for some channels in the 6.7μm water vapor band. Differences should approach zero as the peaks of the channel weighting functions move towards the surface. Non-zero differences appear for window channels because our slanted calculations reproduce the effect of mountains blocking the emission; We recalculate the location of the off-nadir pixel at the intersection of the line-of-sight with the GMAO model terrain. to the projected footprint on the Earth's surface. These effects are also accounted for in our calculations.

Figure 4 is similar to figure 3 but shows the maximum brightness temperature differences of ΔB for each channel. Few profiles produce brightness temperature differences of these magnitudes. For example, approximately 0.0005%(0.003%) of the observations had brightness temperature differences greater than 2(1)K. However, it can be seen that these differences are comparable to or significantly greater than the instrument noise for most AMSU-A channels and many AIRS channels, especially those in the 6.7μm H_2O band and in the most absorbing CO_2 channels in both the 15μm and 4μm bands. The latter channels have tails in their weighting functions that reach into the mesosphere.

The locations of the profiles that produce large differences vary with channel owing to changes in the peaks of the weighting functions and the particular absorber affecting a given channel. Profiles that produce large differences in

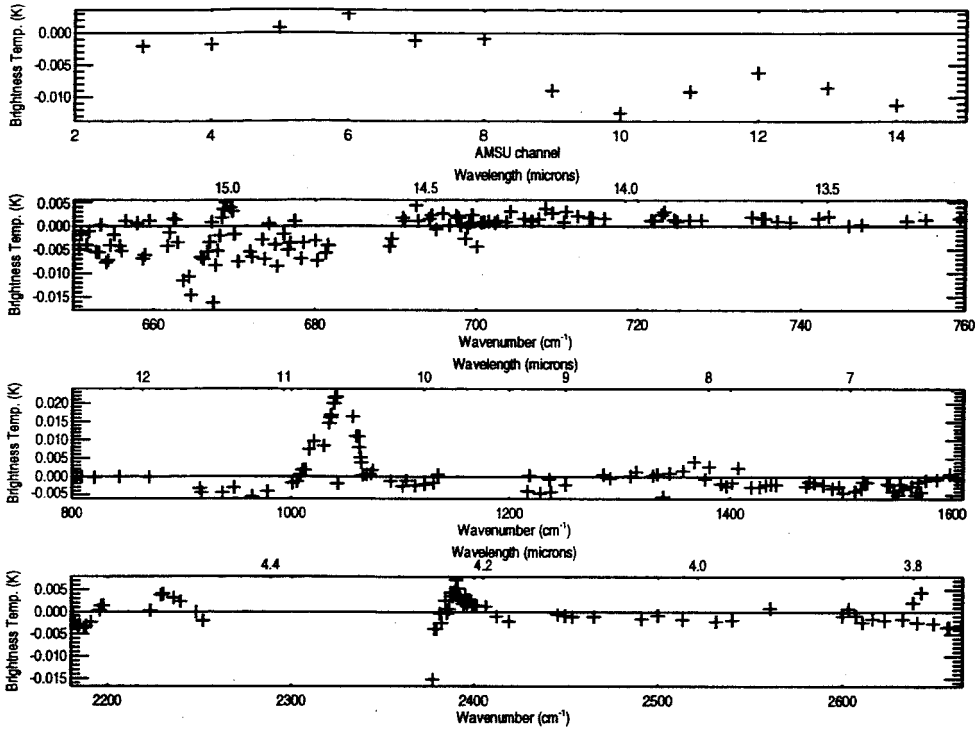

Figure 5. Similar to figure 3 but showing mean values of $\Delta|O-B|$ (+).

7. Summary and Future Work

We have shown that the overall effects of horizontal gradients are relatively small for most AIRS and AMSU-A channels. However, there are a few cases where the effects can be greater than the instrument noise for channels whose weighting functions peak in the upper troposphere and above. The effects are relatively small for the channels that are the most sensitive for numerical weather prediction (middle to lower tropospheric temperature and humidity channels) but are larger for stratospheric temperature channels and the most absorbing AIRS humidity channels in the upper troposphere. Our results suggest that the global analyses used here are capturing gradients well for tropospheric temperature and stratospheric ozone, but less well for upper tropospheric humidity and upper stratospheric and mesospheric temperature where the data used in those analyses is limited. Note that the results obtained here are dependent upon the analyses used and should be repeated in the future when higher resolution or higher quality analyses are available.

The methodology developed here may have applications for other types of nadir-viewing instruments. For example, nadir-viewing ultraviolet and visible radiometers, such as the Ozone Monitoring Instrument (OMI) flying on NASA's EOS Aura, are sensitive to the scattered path of solar photons. Horizontal gradient effects may be particularly important at high solar zenith angles. These conditions typically occur at high latitudes for instruments on polar orbiting satellites where large gradients in ozone can occur at the edges of the polar vortex.

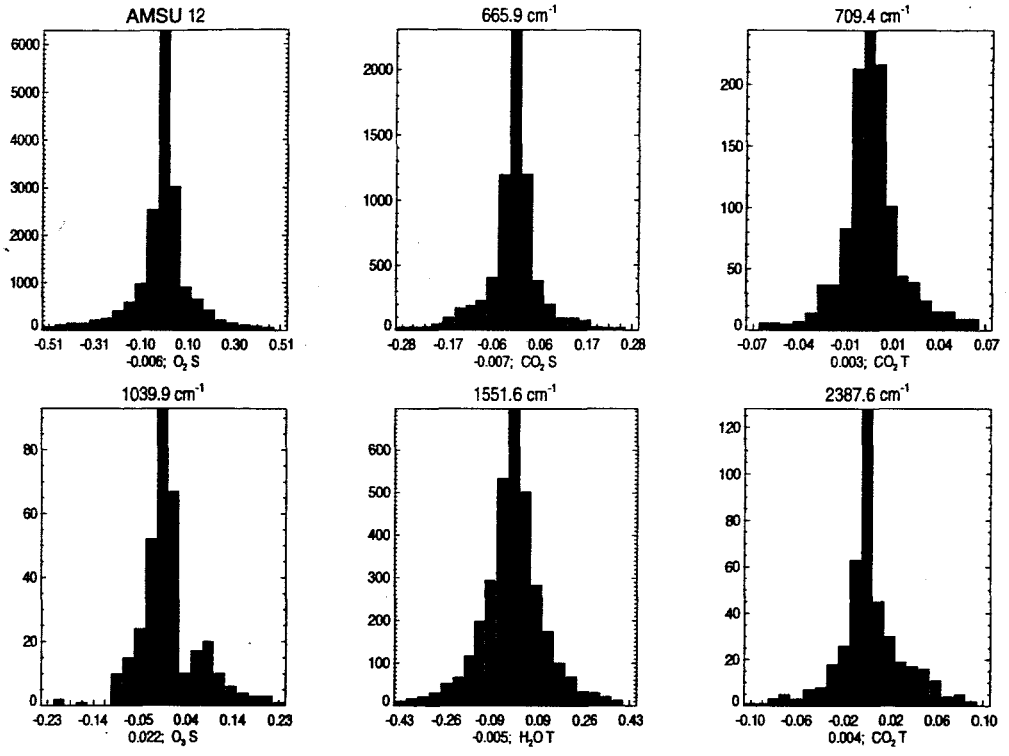

Figure 6. Histograms of $\Delta|O-B|$ for selected channels. The mean value is indicated at the bottom along with the primary absorber and region of absorption, T (S) for troposphere (stratosphere).

We plan to do a similar study for OMI and other UV instruments. The results may have implications for the validation of the total column ozone produced with such instruments including inter-instrument comparisons.

Acknowledgements

The authors thank the AIRS science team, especially M. Goldberg and W. Wolf, for providing the AIRS and AMSU-A data and L. Strow and P. Rosenkrantz for providing the radiative transfer codes. This work was supported by a grant from the National Aeronautics and Space Administration (NASA) through the Joint Center for Satellite Data Assimilation (JCSDA).

References

Aumann, H. H., Chahine, M. T., Gautier, C., Goldberg, M. D., Kalnay, E., McMillin, L. M., Revercomb, H., Rosenkrantz, P. W., Smith, W. L., Staelin, D. H., Strow, L. L., and Susskind, J. 2003 AIRS/AMSU/HSB on the Aqua Mission: Design, science objectives, data products, and processing systems, *IEEE Trans. Geosci. Rem. Sens.*, **41**, 253–264

Cohn S. E., da Silva, A. M., Guo, J., Sienkiewicz, M., and Lamich, D. 1998 Assessing the Effects of Data Selection with the DAO Physical-space Statistical Analysis System, *Mon. Wea. Rev.*, **126**, 2913–2926

Derber, J., and Wu, W.-S. 1998 The use of cloud-cleared radiances in the NCEP SSI analysis system. *Mon. Wea. Rev*, **126**, 2287–2299

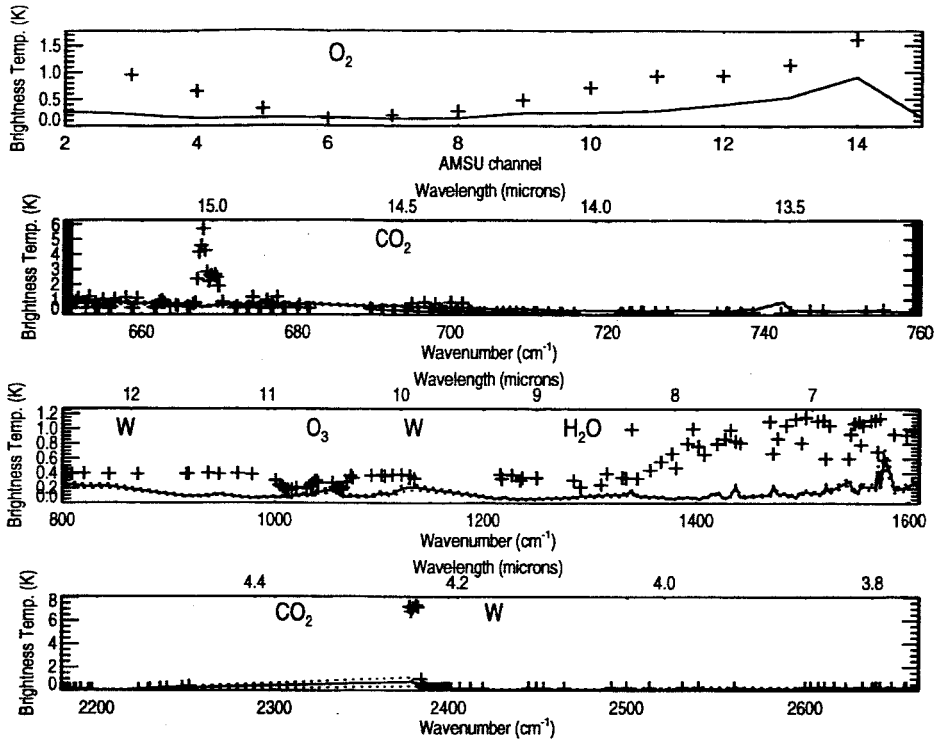

Figure 4. Similar to figure 3 but showing maximum brightness temperature differences (+).

In contrast, we see improvements (positive values) in the lower-peaking tropospheric temperature sensitive channels in both the 15 μm and 4μm bands with the greatest improvements occurring for the higher peaking of these channels. As the weighting functions move towards the surface, the values of ΔB become small because dx as shown in figure 1 goes to zero with dz.

We see the largest improvement in the ozone-sensitive channels. The ozone analysis uses observations from SBUV that are very accurate in the middle to upper stratosphere. It appears that the ozone analysis is providing accurate gradients in ozone that lead to improvements when the slanted atmospheric path is used to compute brightness temperatures.

Figure 6 shows the distributions of $\Delta|O-B|$ for a few representative channels. The histograms indicate that the mean improvement or degradation for a channel is primarily influenced by data in the wings of the distributions. For some channels there are improvements (degradations) near the center of the distributions where the gradient effects are small while the overall mean result was in the opposite direction due to degradations (improvements) in the wings of the distribution where the gradient effects were larger. For example, the stratospheric-peaking AMSU 12 shows improvement near the center of the distribution, but an overall negative mean result. In contrast the lower-peaking AIRS channel with frequency 2387.6 cm^{-1} shows a slight degradation near the center, but an overall positive mean. Note that the differences in the total number of observations for the channels shown result from differences in detected cloud contamination.

Goldberg, M. D., Qu, Y., McMillin, L. M., Wolf, W., Zhou, L., and Divakarla, M.	2003	AIRS Near-real-time products and algorithms in support of operational numerical weather prediction. *IEEE Trans. Geosci. Rem. Sens.*, **41**, 379–389
Joiner, J., Poli, P., Frank, D., and Liu, H. H.	2004	Detection of cloud-affected AIRS channels using an adjacent-pixel approach. *Q. J. R. Meteorol. Soc.*, **126**, 725–748
Kiehl, J. T., Hack, J. J., Bonan, G. B., Boville, B. A., Briegleb, B. P., Williamson, D. L., and Rasch, P. J.	1996	Description of the NCAR Community Climate Model (CCM3). *NCAR Technical Note*, NCAR/TN-420+STR, Boulder, CO, 152pp.
Lin, S.-J.	1997	A finite-volume integration method for computing pressure gradient forces in general vertical coordinates. *Q. J. Roy. Met. Soc.*, **123**, 1749–1762
Poli, P., and Joiner, J.	2004	Effects of horizontal gradients on GPS radio occultation observation operators. Part I: Ray-tracing. *Q. J. R. Meteorol. Soc.*, in press.
Poli, P.	2004	Effects of horizontal gradients on GPS radio occultation observation operators. Part II: A fast atmospheric refractivity gradient operator (FARGO). *Q. J. R. Meteorol. Soc.*, in press.
Rosenkrantz, P. W.	2003	Rapid radiative transfer model for AMSU/HSB channels, *IEEE Trans. Geosci. Rem. Sens.*, **41**, 362–368
Stajner, I., Riishøjgaard, L. P., and Rood, R. B.	2001	The GEOS ozone data assimilation system: specification of error statistics. *Q. J. R. Meteorol. Soc.*, **127**, 1069–1094
Strow, L. L., Hannon, S. E., De Souza-Machado, S., Motteler, H. E., and Tobin, D.	2003	An overview of the AIRS radiative transfer model. *IEEE Trans. Geosci. Rem. Sens.*, **41**, 303–313

User: joiner

airs_tilt.ps

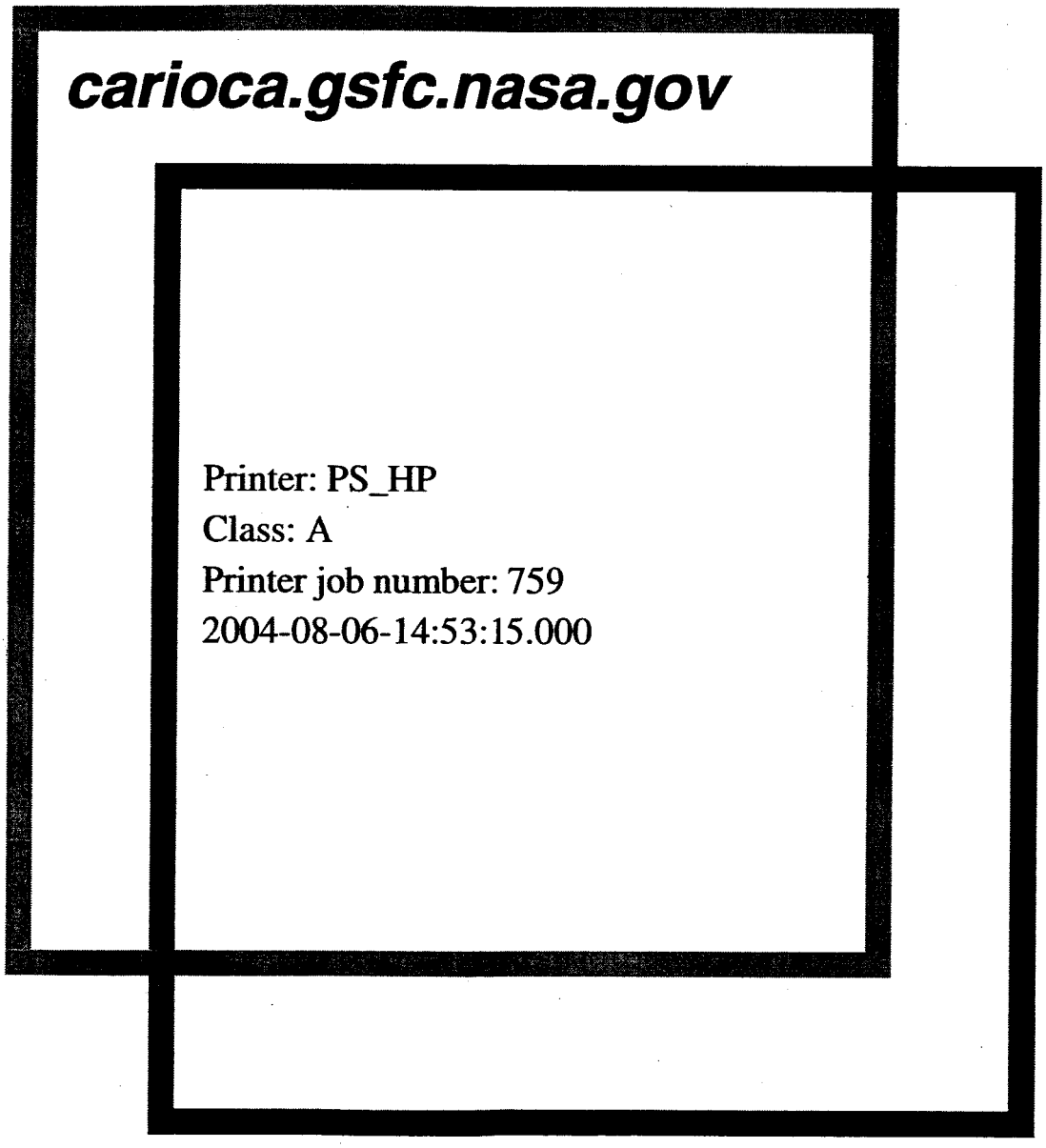

Title: Note on the effect of horizontal gradients for nadir-viewing microwave and infrared sounders

Authors: Joanna Joiner and Paul Poli

To be submitted to the Quarterly Journal of the Royal Meteorological Society

-- POPULAR SUMMARY --

High-spectral resolution infrared and microwave sounders such as the Atmospheric InfraRed Sounder (AIRS) and the Advanced Microwave Sounding Unit (AMSU), flying on NASA's EOS Aqua satellite, provide information about the Earth's vertical temperature and humidity structure. This information may be used to improve forecasts from numerical weather prediction (NWP) systems and to study the Earth's climate. These instruments scan from side to side as the satellite orbits the Earth creating a swath of data below the satellite. At the satellite swath edges, the angle between the vertical at the Earth's footprint location and the satellite can reach about 60 degrees. The measurement made from the satellite is of microwave and infrared radiation that is emitted by the atmosphere and the Earth's surface. At the swath edges, the path of this radiation as it is emitted and absorbed through the atmosphere and observed by the satellite is slanted with respect to the satellite footprint's zenith. Radiative transfer codes currently used to compute the expected radiation use the appropriate slant angle in the calculation. However, typically the input atmospheric fields are those from the vertical profile above the center of the satellite footprint. If horizontal gradients are present in the atmospheric fields, the use of a vertical atmospheric profile may produce an error.

This note attempts to quantify the effects of horizontal gradients on AIRS and AMSU-A channels by computing the expected satellite-observed radiation with accurate slanted atmospheric profiles. We use slanted temperature, water vapor, and ozone fields from the weather prediction systems of NASA's Global Modeling and Assimilation Office (GMAO) and NOAA's National Center for Environmental Prediction (NCEP). We compare the calculations using slanted and vertical profiles with real AIRS and AMSU-A data. We show that the effects of horizontal gradients on these sounders are generally small and below instrument noise. There are cases where the effects are greater than the instrument noise and may produce errors in a weather prediction system. These errors are unlikely to significantly degrade numerical weather forecasts, but they could be significant for other climate applications such as specifying temperature in the stratosphere where ozone loss is occurring.